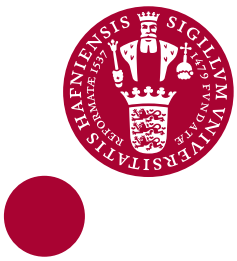

Arabinogalactan glycosyltransferases target to a unique subcellular compartment that may function in unconventional secretion in plants

Poulsen, Christian Peter; Dilokpimol, Adiphol; Mouille, Grégory; Burow, Meike; Geshi, Naomi

Published in:
Traffic

DOI:
10.1111/tra.12203

Publication date:
2014

Document version
Publisher's PDF, also known as Version of record

Traffic

doi:10.1111/tra.12203

Arabinogalactan Glycosyltransferases Target to a Unique Subcellular Compartment That May Function in Unconventional Secretion in Plants

Christian Peter Poulsen[1], Adiphol Dilokpimol[1,5], Grégory Mouille[2,3], Meike Burow[1,4] and Naomi Geshi[1,*]

[1]Department of Plant and Environmental Sciences, Faculty of Science, University of Copenhagen, Thorvaldsensvej 40, Frederiksberg C 1871, Denmark

[2]INRA, Institut Jean-Pierre Bourgin, UMR 1318, ERL CNRS 3559, Saclay Plant Sciences, Versailles F-78026, France

[3]AgroParisTech, Institut Jean-Pierre Bourgin, UMR 1318, ERL CNRS 3559, Saclay Plant Sciences, Versailles F-78026, France

[4]Dynamo Center of Excellence, Faculty of Science, University of Copenhagen, Thorvaldsensvej 40, Frederiksberg C 1871, Denmark

[5]Current address: Fungal Physiology, CBS-KNAW Fungal Biodiversity Center, Uppsalalaan 8, Utrecht 3584 CT, The Netherlands

*Corresponding author: Naomi Geshi, ngeshi@outlook.com

Abstract

We report that fluorescently tagged arabinogalactan glycosyltransferases target not only the Golgi apparatus but also uncharacterized smaller compartments when transiently expressed in *Nicotiana benthamiana*. Approximately 80% of AtGALT31A [*Arabidopsis thaliana* galactosyltransferase from family 31 (At1g32930)] was found in the small compartments, of which, 45 and 40% of AtGALT29A [*Arabidopsis thaliana* galactosyltransferase from family 29 (At1g08280)] and AtGlcAT14A [*Arabidopsis thaliana* glucuronosyltransferase from family 14 (At5g39990)] colocalized with AtGALT31A, respectively; in contrast, *N*-glycosylation enzymes rarely colocalized (3–18%), implicating a role of the small compartments in a part of arabinogalactan (*O*-glycan) biosynthesis rather than *N*-glycan processing. The dual localization of AtGALT31A was also observed for fluorescently tagged AtGALT31A stably expressed in an Arabidopsis *atgalt31a* mutant background. Further, site-directed mutagenesis of a phosphorylation site of AtGALT29A (Y144) increased the frequency of the protein being targeted to the AtGALT31A-localized small compartments, suggesting a role of Y144 in subcellular targeting. The AtGALT31A localized to the small compartments were colocalized with neither SYP61 (syntaxin of plants 61), a marker for *trans*-Golgi network (TGN), nor FM4-64-stained endosomes. However, 41% colocalized with EXO70E2 (*Arabidopsis thaliana* exocyst protein Exo70 homolog 2), a marker for exocyst-positive organelles, and least affected by Brefeldin A and Wortmannin. Taken together, AtGALT31A localized to small compartments that are distinct from the Golgi apparatus, the SYP61-localized TGN, FM4-64-stained endosomes and Wortmannin-vacuolated prevacuolar compartments, but may be part of an unconventional protein secretory pathway represented by EXO70E2 in plants.

Keywords arabinogalactan proteins, exocyst-positive organelle, glycosyltransferase, Golgi apparatus, plant cell walls, protein *O*-glycosylation, proteoglycan biosynthesis, subcellular localization, type II arabinogalactan, unconventional secretory pathway

Received 18 November 2013, revised and accepted for publication 26 July 2014, uncorrected manuscript published online 30 July 2014, published online 12 September 2014

Glycosylation is the major posttranslational modification of proteins and significantly affects protein folding, conformation, distribution, stability and activity. Both *N*- and *O*-glycosylations of proteins are catalyzed by a large numbers of glycosyltransferases (GTs) and glycosidases located in the endoplasmic reticulum (ER) and the Golgi apparatus. The Golgi apparatus is composed of polarized stacks of cisternae, and the bulk flow of the cargo proteins synthesized in the ER moves from *cis* to *trans* Golgi cisternae (reviewed in 1, 2). The *trans*-most cisternae are designated to the *trans*-Golgi network (TGN) and ultimately lead to various post-Golgi organelles to the downstream destinations, such as vacuoles and the plasma membrane.

In eukaryotes, it is thought that proteins secreted to the extracellular space possess an N-terminal signal peptide and are synthesized in the rough ER, transported through the Golgi, TGN and, ultimately, to the plasma membrane. However, many proteins that lack an N-terminal signal peptide are also known to be secreted out of cells (3). In plants, it is estimated that over 50% of the proteins defined in the secretome lack a signal peptide [leaderless secretory proteins (LSPs) (4)]. The process of LSP secretion is referred to as unconventional protein secretion (UPS), and several pathways that foster vesicle-mediated transport or non-vesicle-mediated transport (direct secretion from the cytosol) have been identified in yeast and mammalian cells. In plants, the presence of a pathway independent of a Golgi-mediated secretion process has also been identified by the secretion of two LSPs that are insensitive to the treatment of Brefeldin A [BFA, (5,6)], and recently an 'exocyst-positive organelle' (EXPO) that mediates UPS in plants has been reported (7). EXPO was first identified in suspension-cultured Arabidopsis and tobacco BY-2 cells and possesses distinct features of conventional secretory or endocytic pathways, such as (i) an insensitivity to BFA or Wortmannin and (ii) the inability to uptake FM4-64, an endocytic tracer dye.

In mammalian cells, both *N*- and *O*-glycosylation enzymes are distributed from *cis* to *trans* Golgi cisternae by the natural sequence of the pathway and often form enzyme complexes within each Golgi cisternae (reviewed in (8)). These complexes are considered to be assembly lines needed to produce specific glycoconjugates in an efficient way by substrate channeling. Further, these complexes only seem to form within the same pathway and not across pathways (9), which is a feasible way to organize various pathways that occur simultaneously in a limited space.

Protein *N*-glycosylation is also largely conserved in plants, and a similar arrangement of the enzyme complexes in the Golgi apparatus has been reported (10). Unlike *N*-glycosylation, *O*-glycosylation is not conserved among different organisms and little is known about the organization of *O*-glycosylation enzymes in plants. Arabinogalactan proteins (AGPs), abundant cell-surface proteoglycans present in most plant species examined, are involved in multiple cellular processes, e.g. somatic embryogenesis, cell–cell interactions and cell elongation (11). Glycan is the major component (>90%) of AGPs and is synthesized as a posttranslational modification on the hydroxyproline of proteins in the secretory pathway (*O*-glycosylation). Until recently, little was known about the arabinogalactan (AG) glycosylation process, however, a few of the GTs have recently been identified (12), e.g. AtFUT4/6 *Arabidopsis thaliana* fucosyltransferase 4 and 6 (13), AtGALT2 *Arabidopsis thaliana* galactosyltransferase 2 (14), AtGALT31A [*Arabidopsis thaliana* galactosyltransferase from family 31 (At1g32930)] (15), AtGlcAT14A-C [*Arabidopsis thaliana* glucuronosyltransferase from family 14 (At5g39990)] (16,17) and AtGALT29A [*Arabidopsis thaliana* galactosyltransferase from family 29 (At1g08280)] (18). The occurrence of initial galactosylation on hydroxyprolines was reported to occur in the ER (19), and the fluorescently tagged protein responsible for this reaction (GALT2) is targeted both to ER and to the Golgi when transiently expressed in *Nicotiana tabacum* (14). Similarly, fluorescently tagged AtFUT6 transiently expressed in *N. tabacum* is also found in the Golgi apparatus (13). We reported previously that AtGALT31A, AtGLCAT14A and AtGALT29A are localized to the Golgi apparatus when fluorescently tagged versions of these proteins are expressed transiently in *Nicotiana benthamiana* (15,16,18). Additionally, we reported protein–protein interactions of AtGALT29A and AtGALT31A to form homodimers and heterodimers. We also saw an increase in galactosyltransferase activity by the hetero-enzyme complex when compared with the single enzyme during AGP biosynthesis (18); however, we were unable to detect an interaction between AtGALT31A and AtGLCAT14A (16). Further, little is known about the subcellular localization and protein–protein interactions within *O*-glycosylation enzymes and between *O*- and *N*-glycosylation enzymes in plants.

Because we previously observed that the fluorescently tagged AtGALT31A did not completely colocalize with a Golgi marker protein (15), we investigated the subcellular localization of fluorescently tagged AG GTs (AtGALT31A, AtGLCAT14A and AtGALT29A) in greater detail by statistically analyzing a large number of images. We found that the localization of the AG GTs was not limited to the Golgi apparatus, but was also found to be in uncharacterized smaller compartments. Among the three AG GTs tested, AtGALT31A was most frequently found in the small compartments (ca. 80%) when expressed in *N. benthamiana*,

and a similar dual localization to the Golgi and these smaller compartments was also confirmed for the fluorescently tagged AtGALT31A expressed stably in an Arabidopsis *atgalt31a* mutant background. We report the characterization of these small compartments using fluorescently tagged AtGALT31A as a marker protein in *N. benthamiana* and demonstrate a possibility of a part of AG biosynthesis in an unconventional protein secretory pathway independent of the Golgi-mediated secretory pathway in plants.

Results and Discussion

AG GTs localize frequently to small compartments of approximately 0.5 µm diameter

We investigated the subcellular localization of AG GTs by expressing C-terminal fusion proteins with the monomeric cyan fluorescent protein 3 (mCer3) of AtGALT31A, AtGALT29A and AtGlcAT14A in *N. benthamiana*. *N*-glycan *N*-acetylglucosaminyltransferase I fused to monomeric red fluorescent protein (GnTI-mRFP) (20), *N*-glycan α-mannosidase II fused to monomeric RFP (GMII-mRFP) (21) and sialyltransferase fused to yellow fluorescent protein (ST-YFP) (22) were used as markers for *cis*-, *medial*- and *trans*-Golgi cisternae, respectively. We observed that AtGALT31A-mCer3 was partially colocalized with GnTI-mRFP (Figure 1A–C), GMII-mRFP (Figure 1D–F) and ST-YFP (Figure 1G–I) but was more frequently found in the smaller compartments (as indicated by arrows throughout Figure 1) than in the standard Golgi apparatus of approximately 1 µm diameter where the marker proteins were found (Figure 1). The AtGALT31A-localized small compartments are approximately 0.5 µm diameter in size.

We also observed a similar dual localization of AtGALT31A in *A. thaliana* with a mutant background. When GMII-mRFP was transiently expressed with the T-DNA insertional *atgalt31a* mutant complemented with either N- or C-terminally green fluorescent protein (GFP) tagged AtGALT31A (15), GFP-AtGALT31A (or AtGALT31A-GFP) was found in the smaller compartments as well as in the Golgi apparatus, as defined by GMII (Figure 2 and Figure S1, Supporting Information). Therefore, the dual localization of AtGALT31A-mCer3 in *N. benthamiana*, as shown in Figure 1, is not likely an artifact of transient expression.

Similarly to AtGALT31A-mCer3, AtGALT29A-mCer3 (Figure 3) and AtGlcAT14A-mCer3 (Figure 4) were also found in both the Golgi apparatus, as defined by the marker proteins (GnTI-mRFP, GMII-mRFP and ST-YFP), and in the small compartments (as indicated by arrows, Figures 3 and 4). By comparing the localization of AtGALT31A-mCer, we found that AtGALT29A-mCer3 and AtGlcAT14A-mCer3 were more frequently colocalized with the Golgi markers (overlapped signals in Figures 3 and 4) but were also in small compartments that are approximately 0.5 µm in diameter (as indicated by arrows, Figures 3 and 4), while the Golgi markers were rarely found together in the small compartments.

AtGALT31A colocalizes frequently with EXO70E2, a marker for the EXPO

When we investigated the colocalization of other organelle markers, syntaxin of plants 61 (SYP61) fused to mCer3 [SYP61-mCer3, a marker to TGN, (23)] rarely colocalized with AtGALT31A-YFP (Figure 5A–C). However, AtGALT31A-mCer3 frequently colocalized with EXO70E2 (*Arabidopsis thaliana* exocyst protein Exo70 homolog 2)-GFP, a marker for the EXPO [(7), Figure 5D–F]. Because EXPO is characterized as a part of the UPS (4,7), this result implicates a possibility that these AtGALT31A-localized small compartments are a part of the UPS.

Tyrosine at 144 may control the subcellular targeting of AtGALT29A

Further, we found that amino acid replacement of Tyrosine at 144 (Y144) alters the subcellular targeting of AtGALT29A. The Y144 is predicted to be situated peripherally on the surface of C-terminal globular catalytic domain of AtGALT29A. As phosphorylation of AtGALT29A Y144 has been identified in suspension cells of *A. thaliana* using a proteomics approach [PhosPhAt 4.0; http://phosphat.mpimp-golm.mpg.de/phosphat.html; (24)], we generated Y144A and Y144E AtGALT29A mutant constructs to investigate the significance of the charge status of Y144 in subcellular targeting. As a result, the Y144A AtGALT29A mutant construct less frequently colocalized with a Golgi marker, ST-YFP, when compared with the

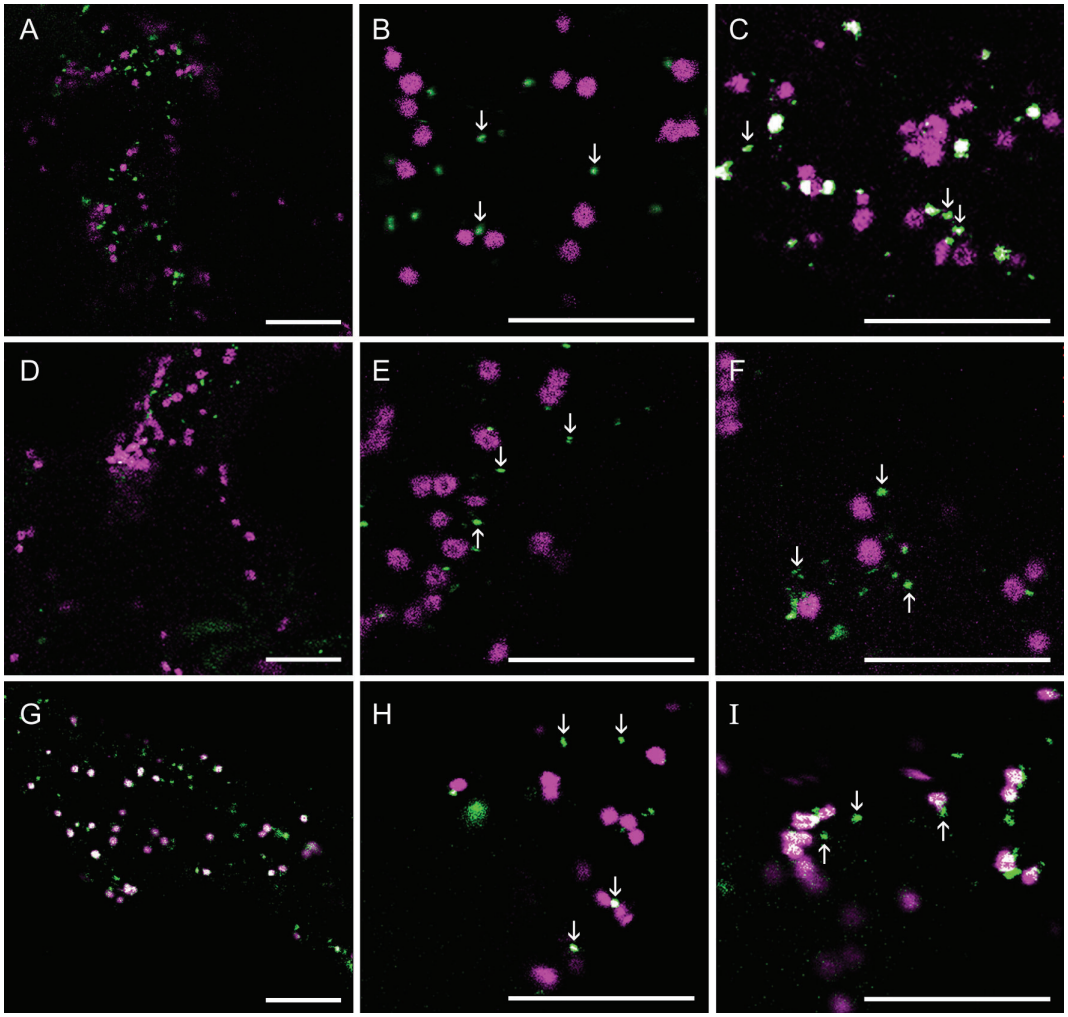

Figure 1: The subcellular localization of AtGALT31A-mCer3. AtGALT31A-mCer3 (A–I, green) was coexpressed with GnTI-mRFP (A–C, magenta), GMII-mRFP (D–F, magenta), and ST-YFP (G–I, magenta) in *N. benthamiana* leaves. AtGALT31A-mCer3 does not always colocalized with GnTI-mRFP and GMII-mRFP but was frequently found in the small compartments, indicated by arrowheads (A–F). AtGALT31A-mCer3 colocalized with ST-YFP (overlapping signals, G–I) but was also often found in the small compartments alone (H–I, indicated by arrowheads). Scale bars = 10 μm.

AtGALT29A wild-type construct (compare Figure 6A,B), and more frequently colocalized with AtGALT31A in the small compartments (Figure 6C, as indicated by arrows). The Y144E AtGALT29A mutant also showed similarly frequent colocalization with AtGALT31A in the small compartments (Figure S2). These results indicate a role of Y144 itself rather than the charge status of Y144 in the subcellular targeting of AtGALT29A. We also investigated involvement of the interaction between AtGALT29A and AtGALT31A in the altered subcellular targeting of Y144A and Y144E AtGALT29A mutant constructs. As previously shown, AtGALT29A-mCer (or -YFP) forms a heterodimer with AtGALT31A-YFP (or -mCer3) (18). The Y144A AtGALT29A-YFP can also form a heterodimer with AtGALT31A-mCer3 as indicated by Förster resonance energy transfer (FRET) (Figure 6D). However, the FRET efficiency (9%) is lower than that found between AtGALT31A-mCer3 and wild-type AtGALT29A-YFP [18%, (18)], suggesting a less frequent dimerization in the case of Y144A. Similarly, Y144E AtGALT29A-YFP also formed a heterodimer with AtGALT31A-mCer3 but with lower FRET efficiency

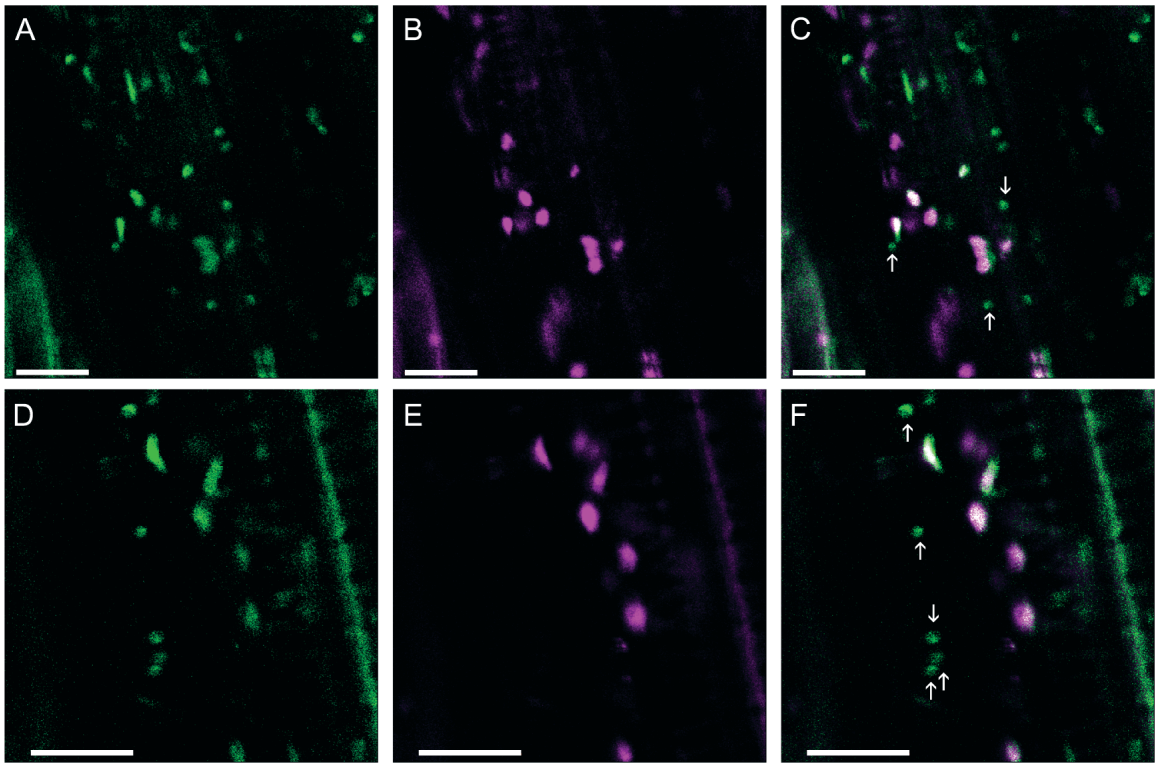

Figure 2: The subcellular localization of GFP-AtGALT31A in the Arabidopsis mutant background. The Arabidopsis T-DNA insertional mutant complemented with a N-terminally GFP tagged construct (GFP-AtGALT31A) was transiently transformed with GMII-mRFP. GFP-AtGALT31A (A, D, green) partially colocalized with GMII-mRFP (B, E, magenta, overlapping signals; C, F), but was also found in the small compartments alone (C, F, indicated by arrows). Similar observation obtained using a C-terminally GFP tagged construct (AtGALT31A-GFP) expressed in the mutant background (Figure S1). Scale bars = 10 μm.

(10%, Figure S2). Therefore, the frequent colocalization of Y144A and Y144E AtGALT29A with AtGALT31A in the small compartments is not likely a result of increased interactions with AtGALT31A, but by some other mechanisms involving Y144 of AtGALT29A.

Distribution of the recombinant proteins in subcellular compartments of 0.9–1.6 or 0.4–0.6 μm diameter

In Figure 7, we summarize the size distribution of the expressed proteins in the subcellular compartments with a diameter of 0.9–1.6 or 0.4–0.6 μm when transiently expressed in *N. benthamiana* and stably expressed in *A. thaliana* in *atgalt31a* background. In the transient expression in *N. benthamiana*, AtGALT31A-mCer3 was most frequently detected in the small compartments (79 ± 5% of the total localization, Figure 7A). AtGALT29A-mCer3, AtGALT29A_Y144A-mCer3 and AtGlcAT14A-mCer3 were also found in the small compartments at a frequency of 25 ± 3, 61 ± 3 and 39 ± 4%, respectively (Figure 7A). The marker proteins for the Golgi apparatus (GnTI, GMII and ST) were also occasionally found in the small compartments (Figure S3) at a frequency of 30 ± 3, 15 ± 2 and 26 ± 4%, respectively (Figure 7A). The TGN as recognized by SYP61 (23) was also recognized as the small compartments (with 82 ± 3% of the total localization, Figure 7A). However, SYP61 rarely colocalized with AtGALT31A (Figure 5A–C), indicating the presence of more than one organelle species in the population of small compartments that are 0.4–0.6 μm in diameter. Upon stable expression in *A. thaliana*, 50 ± 3 and 25 ± 5% of AtGALT31A-GFP and GMII-mRFP was detected in the small compartments, respectively (marked * in Figure 7A). The frequency of localization of AtGALT31A in the small compartments is lower (50 ± 3%) than the protein expressed transiently in *N. benthamiana* (79 ± 5%) and therefore there might be a difference for the subcellular

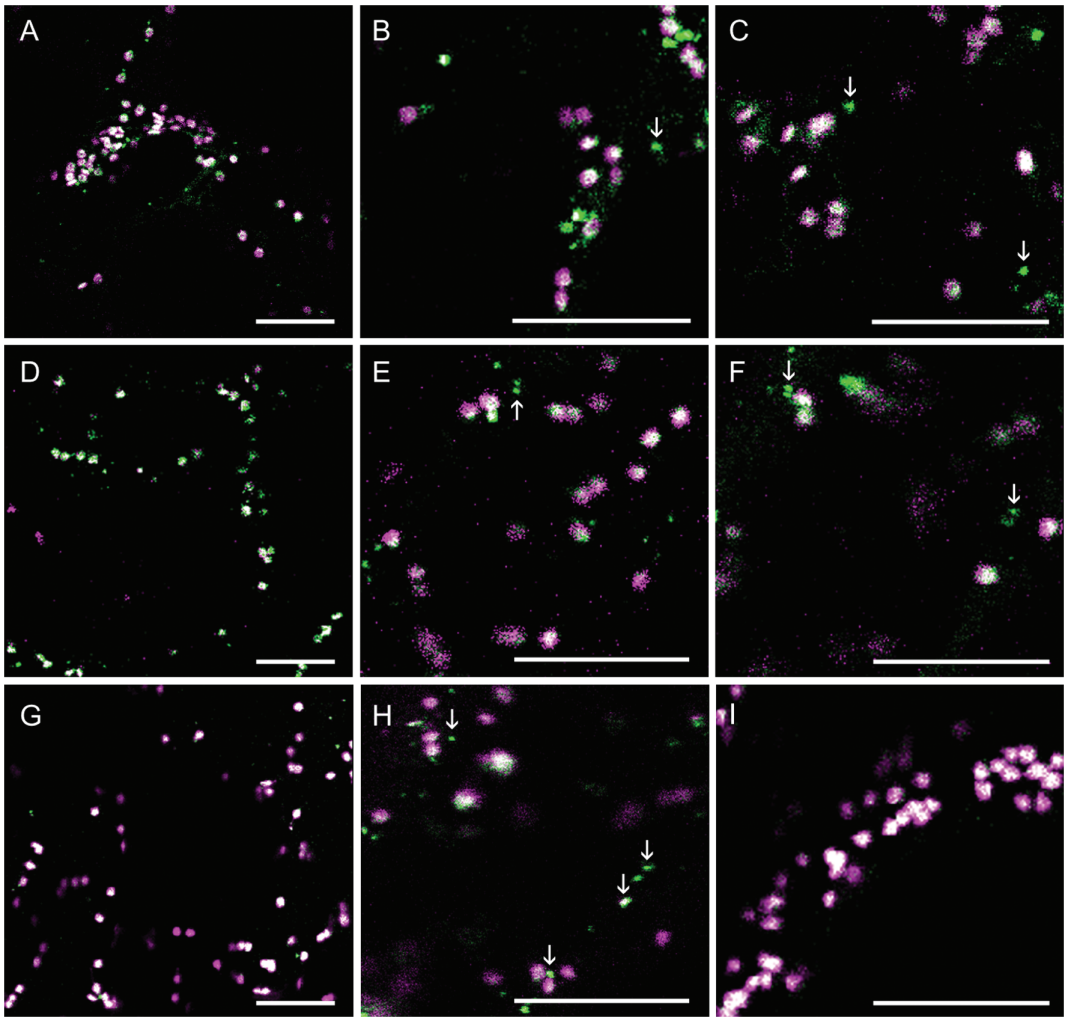

Figure 3: The subcellular localization of AtGALT29A-mCer3. AtGALT29A-mCer3 (A–I, green) was coexpressed with GnTI-mRFP (A–C, magenta), GMII-mRFP (D–F, magenta) and ST-YFP (G–I, magenta) in *N. benthamiana* leaves. AtGALT29A-mCer3 colocalized with GnTI-mRFP, GMII-mRFP and ST-YFP in the Golgi compartments (overlapping signals, A–I) but was also found alone in the small compartments, indicated by arrowheads. Scale bars = 10 μm.

distribution of AtGALT31A expressed in different tissues, plant species, and/or expression method. However, dual localization of AtGALT31A in large and small compartments has been confirmed in both expression systems using *N. benthamiana* and *A. thaliana*.

AtGALT29A, AtGALT14A and EXO70E2 frequently colocalize with AtGALT31A in the compartments of 0.4–0.6 μm diameter

To distinguish the AtGALT31A-localized small compartments from other organelles, we analyzed the colocalization frequency of the proteins of interest with the AtGALT31A-defined small compartments. In transient expression in *N. benthamiana*, a colocalization frequency of 38 ± 8, 66 ± 5 and 42 ± 5% was found for AtGALT29A, AtGALT29A_Y144A and GlcAT14A, respectively, while the colocalization frequency with GnTI, GMII and ST was 18 ± 5, 3 ± 1 and 15 ± 3%, respectively (Figure 7B). In GALT31A stably expressed *A. thaliana atgalt31a*, 9 ± 3% GMII colocalized with GALT31A in the small compartments (marked * in Figure 7B). These results indicate frequent localization of AG GTs in the GALT31A-localized small compartments rather than *N*-glycan GTs. Furthermore, the colocalization frequency with EXO70E2 and

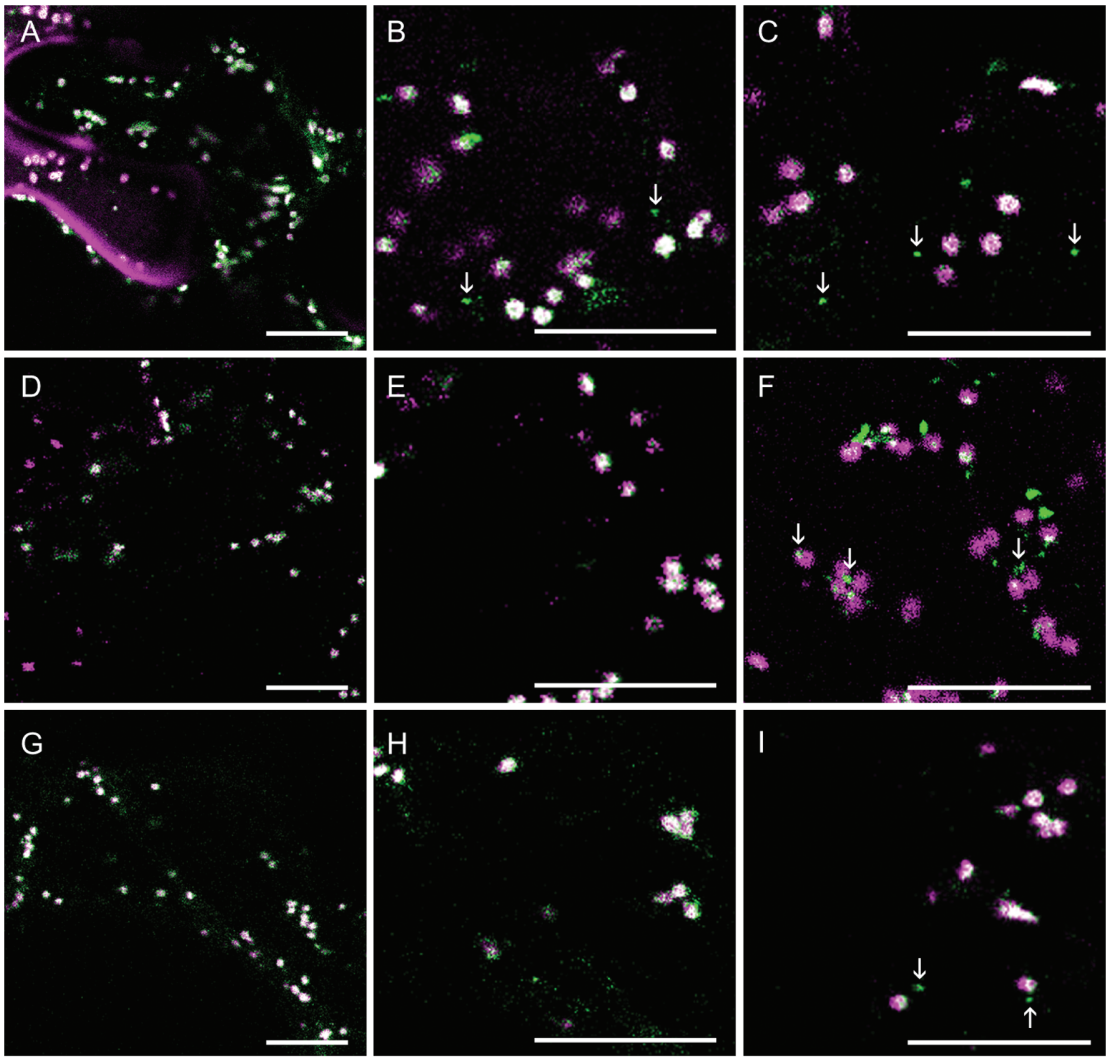

Figure 4: The subcellular localization of AtGlcAT14A-mCer3. AtGlcAT14A-mCer3 (A–I, green) was coexpressed with GnTI-mRFP (A–C, magenta), GMII-mRFP (D–F, magenta) and ST-YFP (G–I, magenta) in *N. benthamiana* leaves. AtGlcAT14A-mCer3 colocalized with GnTI-mRFP, GMII-mRFP and ST-YFP in the Golgi compartments (overlapping signals, A–I) but was also found alone in the small compartments, indicated by arrowheads. Scale bars = 10 μm.

SYP61 was 41 ± 9 and 8 ± 3%, respectively, indicating roughly the same frequency of colocalization of EXO70E2 with AtGALT31A as for the other two AG GTs in the small compartments in *N. benthamiana*. These results support the observations seen in our images (Figures 1–6), namely that a part of the AG biosynthetic pathway seems to be localized to a compartment spatially separated from the Golgi and the TGN, defined by *N*-glycosylation enzymes and SYP61, respectively. Instead, frequent colocalization with EXO70E2 suggests that the AtGALT31A-localized small compartments may be a part of the UPS pathway.

The GALT31A-localized small compartments do not colocalize with FM4-64-stained early endosomes

We characterized the AtGALT31A-localized small compartments further using chemicals, such as FM4-64, BFA and Wortmannin. FM4-64 is used as an endocytic tracer that internalizes and stains early endosomes (25–28). We investigated the colocalization of the AtGALT31A-localized small compartments and the early endosome stained by the internalized FM4-64 (25–28) and compared with the SYP61-localized TGN. In the *N. benthamiana* leaves used in this study, we observed a clear internalization

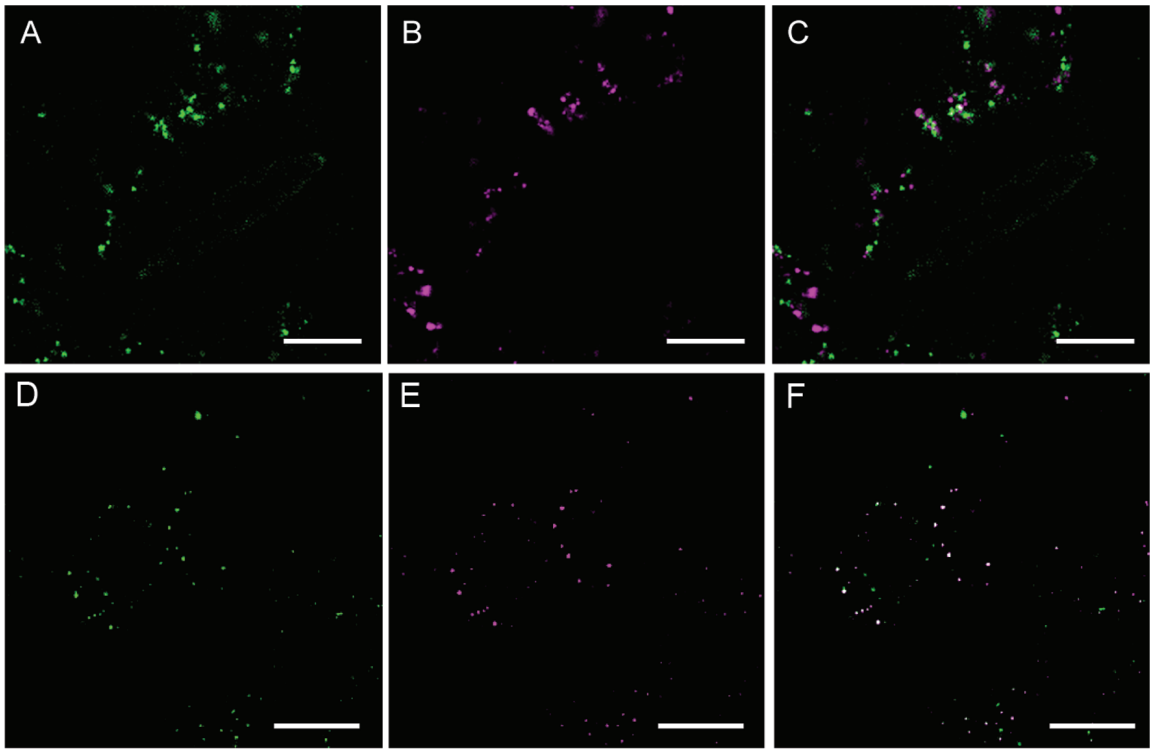

Figure 5: Analysis of AtGALT31A-YFP-localized small compartments. AtGALT31A-YFP (A, green) did not colocalize with the SYP61-mCer3-localized TGN subdomain (B, magenta) (C, overlapped image of A and B), while AtGALT31A-mCer3 (D, green) frequently colocalized with EXO70E2-GFP (E, magenta), a marker for the exocyst-positive organelle (EXPO) (F, overlapped image of D and E). Scale bars = 10 μm.

of FM4-64, which demonstrated a sequential staining from the plasma membrane, internal compartments, and aggregation of the compartments over time (Figure 8). In this condition, the AtGALT31A-localized small compartments were not colocalized with the FM4-64-stained compartments for up to 140 min (Figure 8A–C). We had intended to use SYP61 as a positive marker for the colocalization with the FM4-64-stained early endosomes (29–32), however, we observed that SYP61-containing TGN subdomains did not colocalize with FM4-64-stained compartments for up to 140 min (Figure 8D–F). The reason for this discrepancy with the previous reports remains unknown. However, FM4-64 clearly worked properly in our conditions; therefore, this difference may be due to the definition of TGN domains by different markers. Most of the published studies for TGN have been performed using VHA-a1 as a marker, but the distinct properties of the TGN subdomains as defined by VHA-a1 or SYP61 expressed in *N. benthamiana* leaves have been previously reported (33). Additionally, the TGN in *N. benthamiana* leaves characterized in this study may have slightly different properties than the TGN in the Arabidopsis root used in most of the prior publications. This variation can be implicated by the different properties of the Golgi apparatus and the TGN in response to BFA and its analogue from different plant species and tissues as reported in (34). Nevertheless, under the experimental conditions used in this article, the AtGALT31A-localized small compartments did not colocalize with the FM4-64-stained compartments for up to 140 min (Figure 8A–C), indicating an exclusion of the AtGALT31A-localized small compartments from the endocytic pathway followed by FM4-64.

The AtGALT31A-localized small compartments are least affected by BFA and Wortmannin treatments

Next, we investigated the AtGALT31A-localized small compartments for a response to the treatment with BFA and Wortmannin, both of which are two well-studied

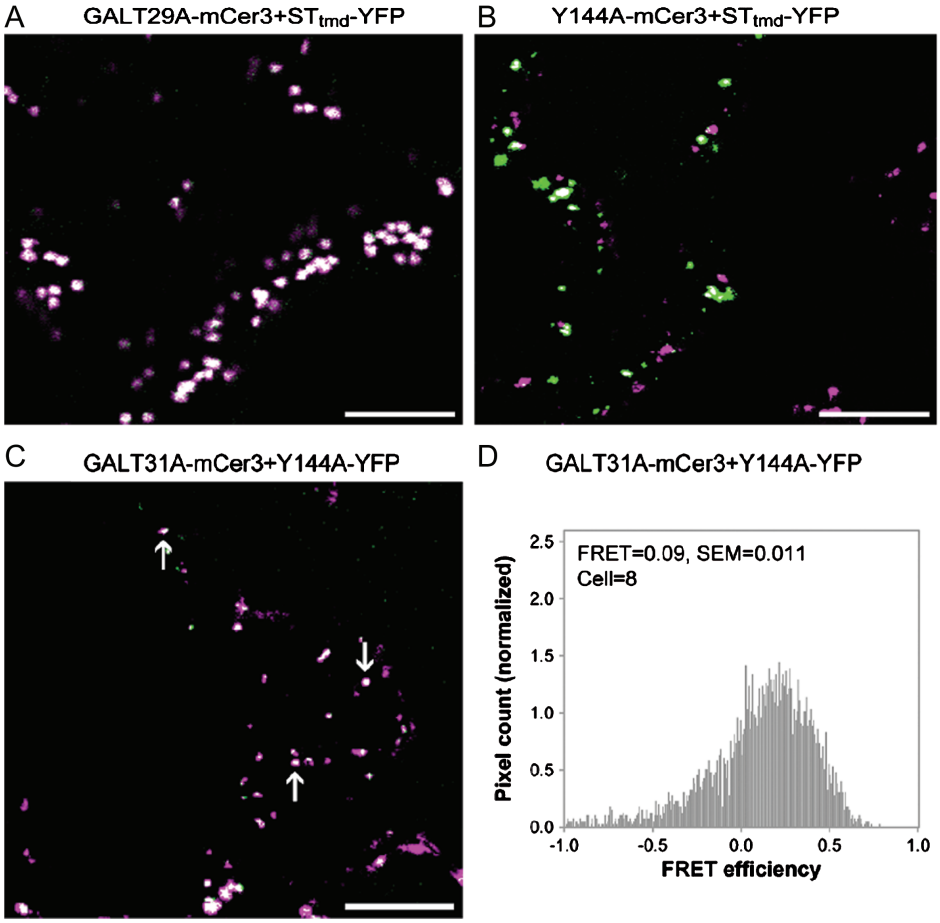

Figure 6: The subcellular localization of AtGALT29A wild-type and Y144A mutant. Overlaid images of AtGALT29AmCer3 (A, green) and STtmd-YFP (A, magenta), Y144A-mCer3 (B, green) and STtmd-YFP (B, magenta), or AtGALT31A-mCer3 (C, green) and Y144A-YFP (C, magenta) transiently expressed in *N. benthamiana* leaves. Scale bars = 10 μm. The image of AtGALT29A-mCer3+ STtmd-YFP (A) was obtained from (17) and is shown here as a reference for comparison. Distribution histograms for pixel by pixel analysis of FRET between AtGALT31A-mCer3 and Y144A-YFP (D). A FRET value = 0.09 translates to a FRET efficiency of 9%; SEM indicates standard error of means; cell indicates number of cells analyzed.

drugs affecting different steps of vesicle trafficking in the secretory pathway.

BFA blocks vesicle trafficking by a rapid release of Coat protein I (COPI) to the cytosol (35), which results in a loss of Golgi cisternae (36) and a formation of the BFA body and aggregates (37–40). The response to BFA treatment was compared with TGN and Golgi as defined by SYP61 and ST, respectively (Figure 9). The effect of BFA became apparent in the TGN and Golgi after 30 min (Figure 9F,J), at which point organelle aggregation and retrograde trafficking back to ER were both observed. This result was consistent with the previous reports (29,41,42). However, AtGALT31A-localized small compartments were rarely affected by BFA for up to 60 min (Figure 9B,C) and the organelle aggregation began to be observed after 150 min (Figure 9D). The difference can be observed more clearly when AtGALT31A and ST were coexpressed (Figure 9M–P): ST-localized Golgi lost its punctate structure after 30 min, while GALT31A-localized small compartments kept the structure up to 150 min after BFA treatment. Clearly, the AtGALT31A-localized small compartments are insensitive to the BFA treatment compared with the Golgi apparatus and the TGN as defined by ST and SYP61, respectively. Insensitivity toward BFA treatment is a definition of the UPS pathway (4), hence the result

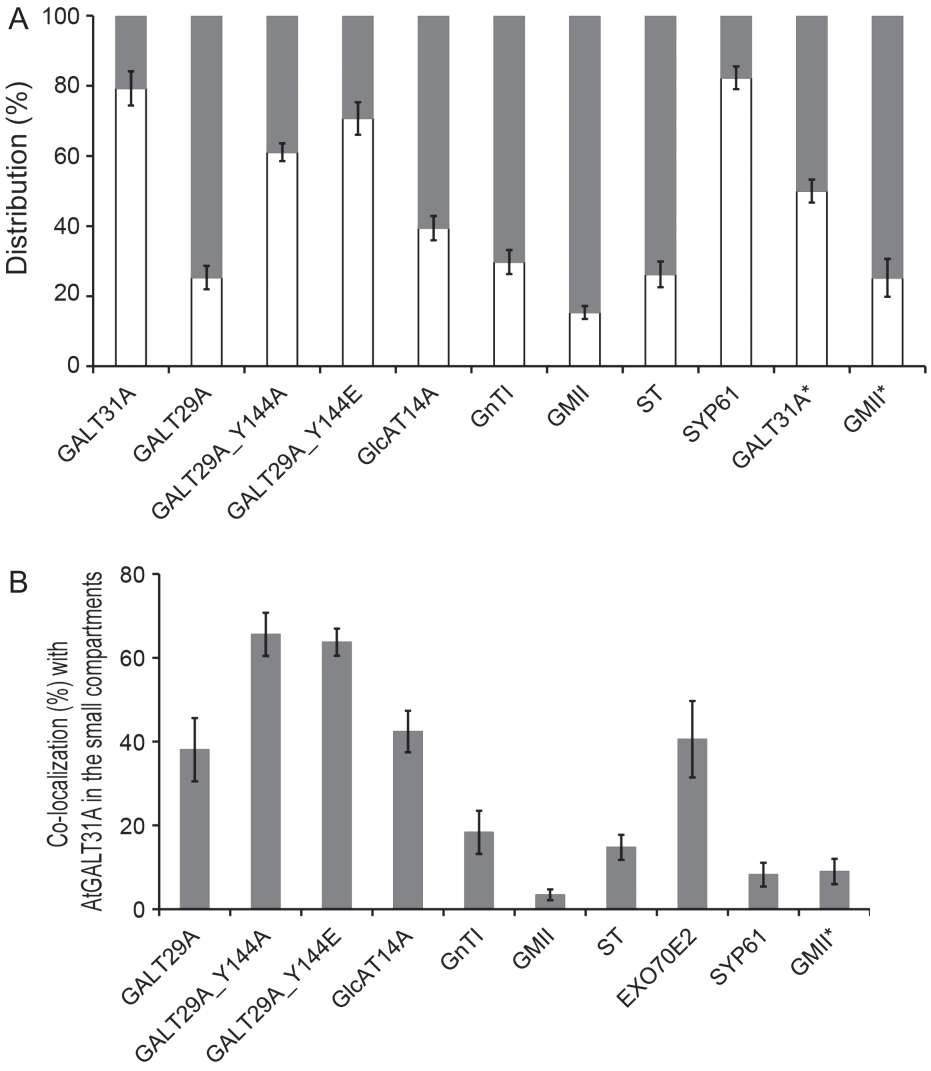

Figure 7: Analyses of the subcellular localization of proteins expressed in *N. benthamiana* leaves or expressed in *A. thaliana atgalt31a* seedlings root (marked *). A) Distribution of the proteins was analyzed by the size of subcellular compartments, namely a diameter of 0.4–0.65 μm (empty bar) or 0.9–1.6 μm (filled bar, the latter corresponds to the standard Golgi stacks). The number of proteins localized in compartment of either size was counted and presented as % distribution. Subcellular compartments of 403–955 from 13–22 cells were used for the analysis. B) Colocalization frequency of the expressed proteins within the AtGALT31Alocalized small compartments (0.4–0.65 μm). Among the signals found in the small compartments, (A), is the colocalization frequency together with AtGALT31A calculated and presented as % distribution. Error bars indicate standard error of mean (SEM) for % distribution among cells analyzed. SYP61, a marker for trans-Golgi network; Exo70E2, a marker for an exocyst-positive organelle.

indicates the AtGALT31A-localized small compartments as a part of the UPS pathway.

Wortmannin is an inhibitor of phosphatidylinositol-3 kinase, and treatment with Wortmannin causes swelling and vacuolation of prevacuolar compartments (PVCs) (41,43) and impairs endocytosis from the plasma membrane (41). The TGN subdomains labeled with VHA-a1 or syntaxin of plants 41 (SYP41, a plant ortholog of yeast TLG2) (32), RAB-A1c (44) or YPT/RAB GTPase interacting protein 4 [YIP4, (45)] have been reported as Wortmannin-insensitive in Arabidopsis root cells. We tested the response of AtGALT31A-localized small compartments toward Wortmannin treatment and

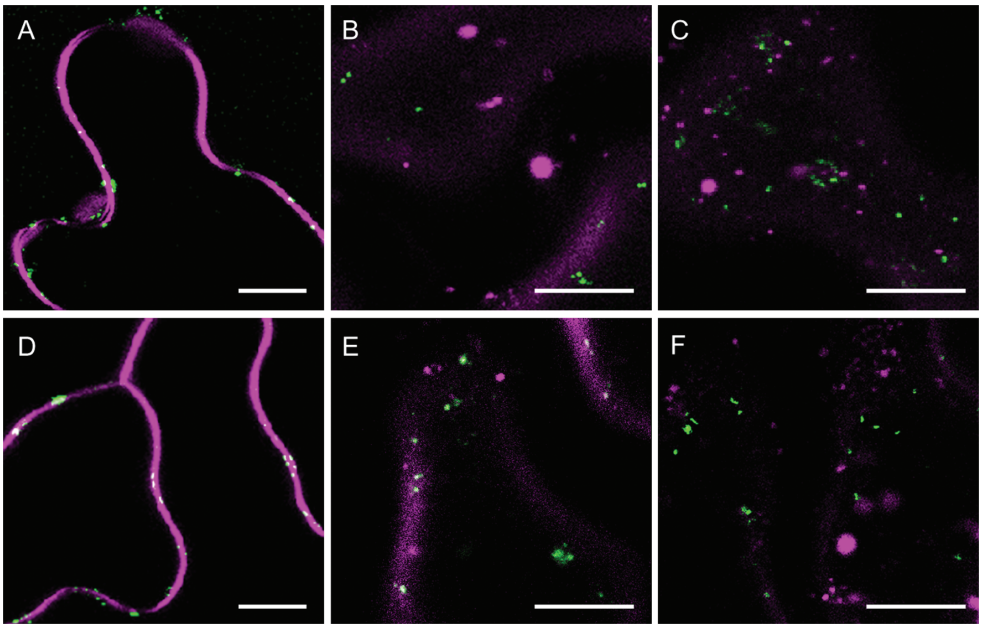

Figure 8: Trace of FM4-64 via endocytosis and AtGALT31A-localized small compartments. Images were taken at 10 min (A, D), 40 min (B, E) and 140 min (C, F) after application of FM4-64 to AtGALT31A-mCer3 or SYP61-mCer3 expressed *N. benthamiana* leaves. Both AtGALT31A-mCer3-localized compartments (A–C, green) and SYP61-mCer3-localized TGN subdomains (D–F, green) were not colocalized with the FM4-64-internalized early endosome and its aggregates (magenta) up to 140 min. Scale bars = 10 μm.

compared this to the SYP61- and ST-localized TGN and Golgi apparatus, respectively. The treatment was performed in the presence of FM4-64 (Figure 10). The FM4-64-stained early endosome formed characteristic ring structures upon Wortmannin treatment at 40 min (Figure 10C,G,K), which is consistent with previous reports (46,45). However, all other compartments defined by AtGALT31A-mCer3, SYP61-mCer3 and ST-CFP were excluded from the ring structures at 40 min of treatment (Figure 10C,G,K). A merger of the ring structure was first observed at 100 min for both AtGALT31A-localized small compartments and SYP61-TGN (Figure 10D,H), while ST-localized Golgi was still excluded at 100 min (Figure 10L). The result indicates the GALT31A-localized small compartments are rather insensitive to Wortmannin and the response is similar to the SYP61-mCer3-localized TGN.

Collectively, the AtGALT31A-localized small compartments are distinct from the Golgi apparatus, TGN, early endosome and PVC in terms of colocalization with the respective markers and a response toward BFA and Wortmannin. Insensitivity to BFA is an indication of a transport pathway that by-passes the Golgi apparatus, namely the UPS pathway (4). When also considering their colocalization with EXO70E2, a marker for EXPO, AtGALT31A-localized small compartments may also be a part of the UPS pathway in plants.

Conclusion and future perspectives

AGP biosynthesis initiates in the ER and continues in the Golgi apparatus. This article presented data demonstrating that at least some of the *O*-glycosyltransferase proteins (AGP biosynthesis) are localized to a subcellular compartment different from Golgi apparatus. On the basis of colocalization with marker proteins as well as a response toward inhibitors of vesicle trafficking, these unique compartments are distinct from the Golgi, SYP61-TGN subdomains, early endosomes and PVC but may be a part of the UPS pathway represented by EXPO defined by EXO70E2. In mammalian cells, both *N*-and *O*-glycosyltransferases are colocalized to the Golgi cisternae but are distinct from each other through the formation of separate protein complexes. In plant cells, the formation of protein complexes is also reported for

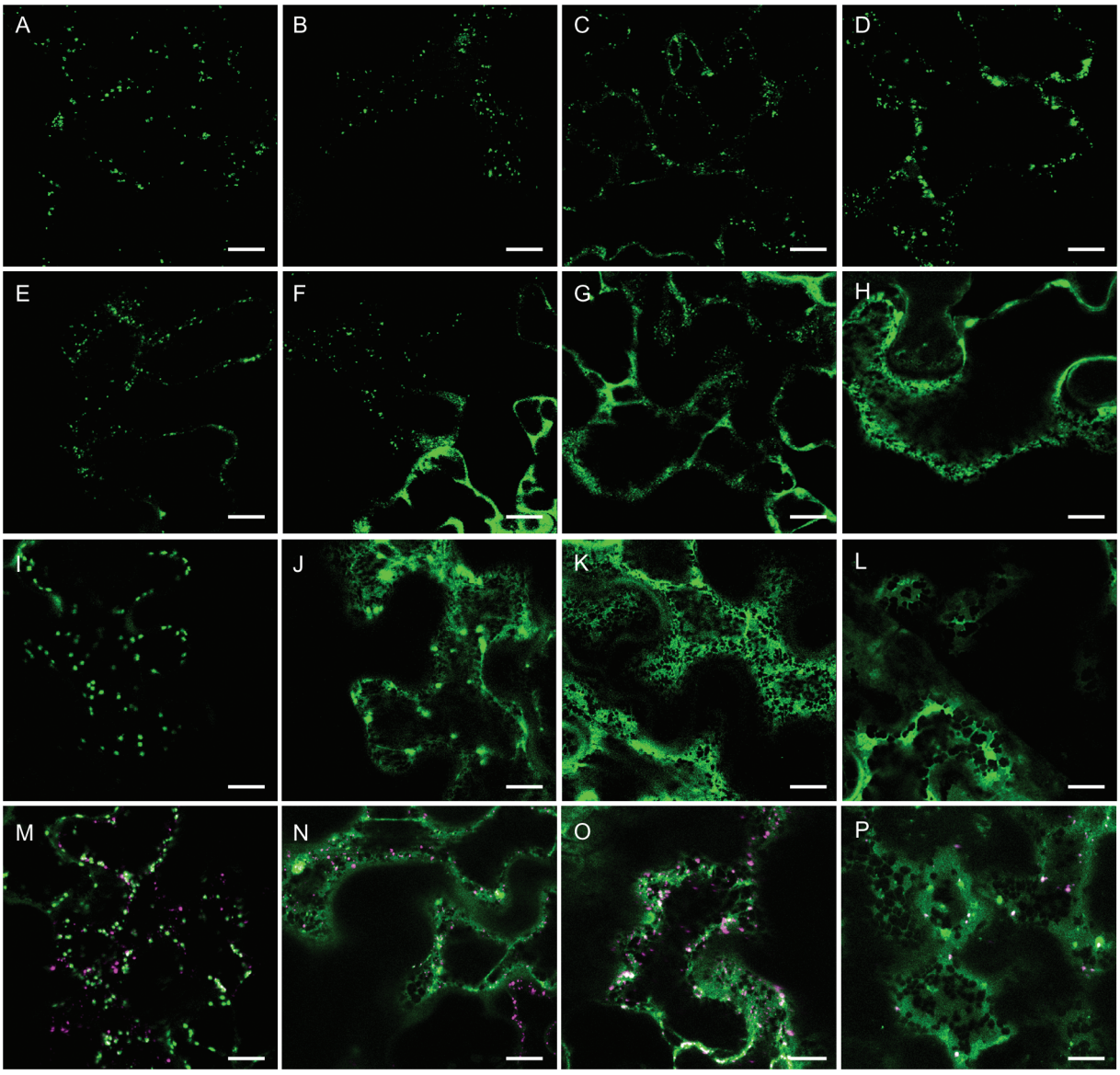

Figure 9: The effect of BFA treatment. AtGALT31A-mCer3 (A–D), SYP61-mCer3 (E–H) and ST-CFP (I–L) singly expressed or AtGALT31A-YFP and ST-CFP coexpressed (M–P; YFP in magenta, CFP in green) in *N. benthamiana* leaves was treated with BFA for 0 min (A, E, I, M), 30 min (B, F, J, N), 60 min (C, G, K, O) and 150 min (D, H, L, P). The effect of BFA appeared already at 30 min for TGN and Golgi stacks defined by SYP61-mCer3 (F) and ST-YFP (J), respectively, while a similar effect was first observed at 150 min for AtGALT31A-mCer3-localized compartments (D). The difference was clearer in the coexpressed images of AtGALT31A-YFP and ST-CFP (M–P): where the effect of BFA to Golgi stacks defined by ST-CFP already appeared at 30 min (N, green), while punctated images of compartments defined by AtGALT31A-YFP were still observed at 150 min after the treatment (P, magenta). Scale bars = 10 μm.

N- and *O*-glycosylation enzymes (10,18), additionally, there may be an additional level of organization (localization to spatially distinct compartments) for both *N*- and *O*-glycosylation enzymes in plant cells.

Our results arise questions for future investigation of: (i) the origin of the AtGALT31A-localized small compartments, (ii) the relation of the small compartments to Golgi and EXPO in (*O*-glyco)protein secretion, (iii)

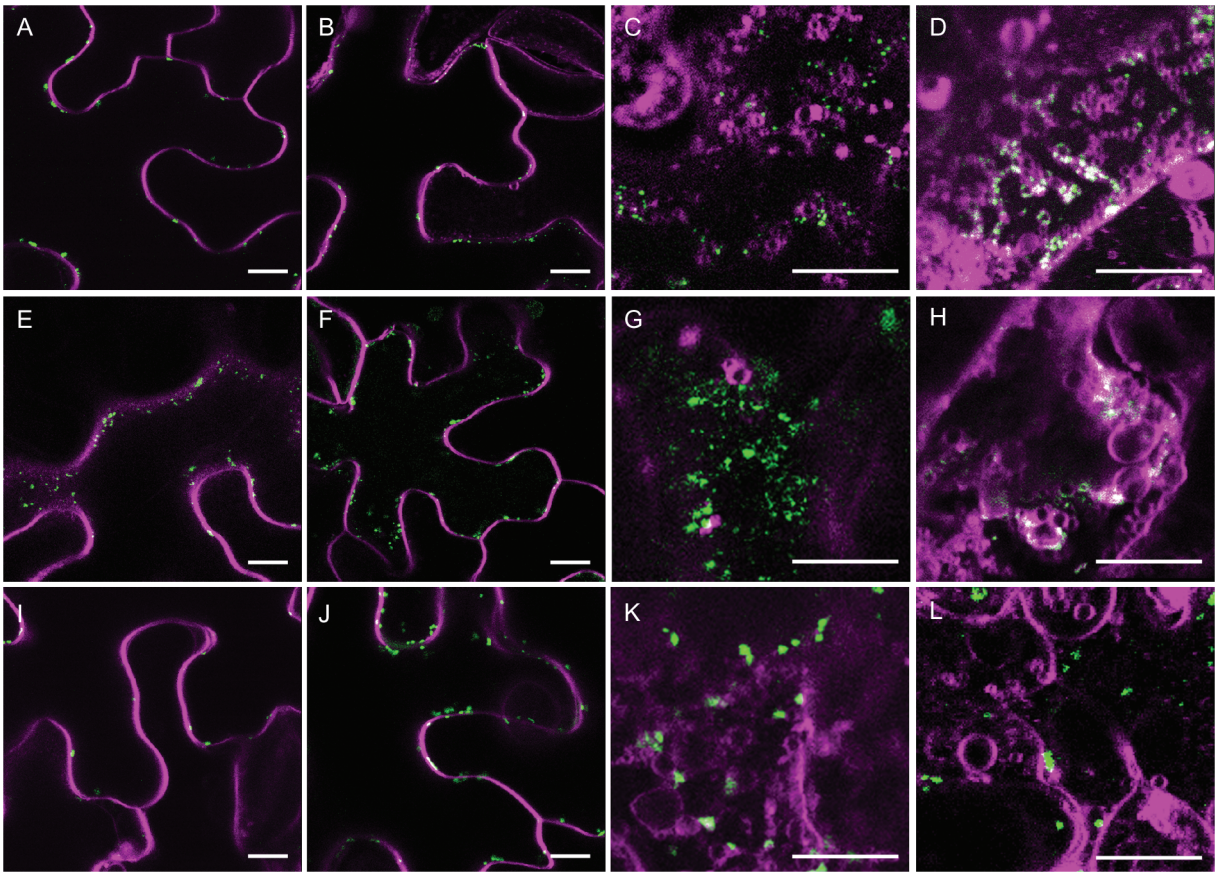

Figure 10: The effect of Wortmannin treatment. AtGALT31A-mCer3 (A–D), SYP61-mCer3 (E–H) and ST-CFP (I–L) (green) expressed *N. benthamiana* leaves was cotreated with Wortmannin and FM4-64 (magenta) for 0 min (A, E, I), 20 min (B, F, J), 40 min (C, G, K) and 100 min (D, H, L). Merger of the AtGALT31A compartments and SYP61-localized TGN to FM4-64 compartments appeared at 100 min (D and H), while the Golgi stack defined by ST-CFP was not merged to FM4-64 compartments at 100 min (L). Scale bars = 10 μm.

targeting and distribution mechanisms of GTs between Golgi and the small compartments and (iv) regulatory and retaining mechanisms of (iii). The obtained knowledge offers novel tools for the recombinant production of high-value compounds using plant protein secretion pathway(s) (47).

Materials and Methods

Materials

EXO70E2-GFP (*At5G61010*) cloned into the pBI221 vector (7) was kindly provided by Dr. Liwen Jiang, School of Life Sciences, Centre for Cell and Developmental Biology, Chinese University of Hong Kong, China. YFP-SYP61 (*AT1G28490*) cloned into the pDS13 vector (48) was kindly provided by Dr. David Robinson, in the Department of Plant Cell Biology Centre for Organismal Studies, University of Heidelberg, and used as a template for further cloning. DNA constructions for the first 77 N-terminal amino acids (CTS region) of *N. tabacum* β1,2-*N*-acetylglucosaminyltransferase I fused to mRFP [GnT1-mRFP, (42)] and the first 52 N-terminal amino acids of the *A. thaliana* α-mannosidase II fused to mRFP [GMII-mRFP, (42)] were kindly provided by Dr. Richard Strasser, University of Natural Resources and Life Sciences-BOKU, Austria.

DNA constructs

Y144A and Y144E AtGALT29A mutant constructs were generated by site-directed mutagenesis by polymerase chain reaction (PCR) using primer pairs of Y144A-sense: CTCGTAGAAGAGCT*GCT*GAACCTAAT ATC; Y144A-antisense: GATATTAGGTTC*AGC*AGCTCTTCTACGAG; Y144E-sense: CTCGTAGAAGAGCT*GAG*GAACCTAATATC; Y144E-antisense: GATATTAGGTTC*CTC*AGCTCTTCTACGAG (mutation positions indicated by italicization) using AtGALT29A-pDONR223 (18)

as a template. Mutant plasmids were transformed to *Escherichia coli* DH10B, verified by sequencing, and moved to the Gateway expression vectors [pEarleyGate mCer3, pEarleyGate 101, (16,49)] using LR reaction (Life Technologies).

Full length SYP61 cDNA without a stop codon was cloned into the Gateway entry vector (pDONR223) by PCR using the sense primer, 5′-GGGGACAAGTTTGTACAAAAAAGCAGGCTTCATGTCTTCAG CTCAAGATCC-3′, the antisense primer, 5′-GGGGACCACTTTGTAC AAGAAAGCTGGGTGTTAGGTCAAGAAGACAAGAACGAATAGG-3′ and the YFP-SYP61 in pDS13 as a template, followed by the BR reaction (Life Technologies). The entry clones were verified by sequencing, and moved to the Gateway expression vectors [pEarleyGate mCer3, pEarleyGate 101, (16,49)] using LR reaction (Life Technologies). DNA constructs for *A. thaliana* galactosyltransferase from family GT31 [AtGALT31A-mCer3, (15)], *A. thaliana* galactosyltransferase from family GT29 [AtGALT29A-mCer3, (18)] and *A. thaliana* glucuronosyltransferase from family GT14 [AtGlcAT14A-mCer3, (16)] are described in the indicated publications.

Expression of recombinant proteins in *N. benthamiana* and image acquisition

Expression constructs were transformed into the *Agrobacterium tumefaciens* strain C58C1 pGV3850. Agrobacteria-mediated transient transformation of *N. benthamiana* leaves was carried out according to (16). The infiltration of Agrobacterium strains harboring the appropriate construct ($OD_{600} = 0.2$) was performed together with the strain harboring the *p19* construct ($OD_{600} = 0.1$). Image acquisition was performed with a Leica SP5 confocal laser scanning microscope (Leica Microsystems GmbH) equipped with a 63× objective lens using the settings described in 50.

Transient expression in Arabidopsis thaliana

Complementation of the Arabidopsis T-DNA insertional mutant *atgalt31a* (*At1g32930*, FLAG_379B06) with AtGALT31A cDNA fused to either N-terminal GFP in pGWB6 (35S:GFP-AtGALT31A) or C-terminal GFP in pGWB5 (35S:AtGALT31A-GFP) was previously described (15). The seeds of the complemented lines were surface-sterilized, plated on 0.5× Murashige and Skoog (MS) medium including vitamins (Duchefa Bio), pH 5.8, supplemented with 1% (w/v) sucrose and cold-stratified. Seedlings were grown at 80–120 μE/(m^2 second), 16 h light and 20°C for 4 days. The cocultivation steps were modified based on previously published protocols (51,52). In brief, 30–40 seedlings were submerged in 1 mL of *Agrobacterium tumefaciens* GV3101, $OD_{600} = 2.5$ in cocultivation medium [0.25× MS containing 1% (w/v) sucrose, 100 μM acetosyringone, 0.005% (v/v) Silwet L-77 and 5 mM MES pH 5.8] for 20 min, transferred to a stack of filter paper soaked in cocultivation medium and then incubated at 80-120 μE/(m^2 second) and 20°C for approximately 40 h. The top filter paper with the seedlings was moved to 0.25× MS agar plates containing 1% (w/v) sucrose and 500 mg/L carbenicillin and the plates were kept at room temperature overnight.

Treatments with FM4-64, BFA and Wortmannin

Infiltration of *N. benthamiana* leaves with 50 μM FM4-64 dye [*N*-(3-Triethylammoniumpropyl)-4-(6-(4-(Diethylamino) Phenyl) Hexatrienyl);Life Technologies] followed the method described in (53). Infiltration with 40 μM Wortmannin (Sigma-Aldrich) was performed by coinfiltration with 50 μM FM4-64 (53). BFA (3.5 mM) treatment was performed by agitating the leaf disk in the solution as described in (42). Images from different time points of the respective treatment were acquired using a Leica SP5 confocal laser scanning microscope (Leica Microsystems GmbH).

Image analysis

For the analyses of vesicle distribution and colocalization frequency, the images were thresholded, converted to binary, and signals with a circularity between 0.2 and 1 were defined using the 'analyze particles' function available in the ImageJ software [U.S. National Institutes of Health; (54)]. The fluorescent signals were grouped into two categories according to the area, either between 0.13 and 0.33 μm^2 or 0.64 and 2.01 μm^2, each of which corresponds to a circle with the diameter of 0.4–0.65 or 0.9–1.6 μm, respectively. Colocalization frequency was analyzed by defining all AtGALT31A-localized small compartments (channel 1) in the cells coexpressing with AtGALT29A, AtGlcAT14A, GnTI, GMII or ST (channel 2). The AtGALT31A-localized small compartments (channel 1) that also contained the signal from channel 2 in a minimum 20% of the area were judged as 'colocalized'.

Acknowledgments

This work was supported by the Danish Council for Strategic Research, Food, Health and Welfare (09-067059) and the Danish Council for Independent Research, Technology and Production Sciences (274-09-0113) with a grant to N. G. Imaging data were collected at the Center for Advanced Bioimaging (CAB) Denmark, University of Copenhagen.

Supporting Information

Additional Supporting Information may be found in the online version of this article:

Figure S1: The subcellular localization of AtGALT31A-GFP in the Arabidopsis mutant background. The Arabidopsis T-DNA insertional mutant complemented with a C-terminally GFP tagged construct (AtGALT31A-GFP) was transiently transformed with GMII-mRFP. AtGALT31A-GFP (A, green) partially colocalized with GMII-mRFP (B, magenta, overlapping signals; C), but was also found in the small compartments alone (C, indicated by arrows), which is similar to the observation obtained using an N-terminally GFP tagged construct (GFPAtGALT31A) expressed in the mutant background (Figure 2). Scale bars = 10 μm.

Figure S2: Subcellular localization and FRET analysis of Y144E AtGALT29A transiently coexpressed with AtGALT31A in *N. benthamiana* leaf. A) The overlaid images of AtGALT31A-mCer3 (green) together with Y144E AtGALT29A-YFP (magenta) are presented. Some of the colocalized images are indicated (arrows). Scale bar = 10 μm. B) Distribution histograms for pixel by pixel analysis of FRET between AtGALT31A-mCer3 and Y144E AtGALT29A-YFP. A FRET value = 0.10 translates to a FRET efficiency of 10% FRET. SEM indicates standard error of means; Cell indicates number of cells analyzed.

Figure S3: Localization of *N*-glycan GTs in small vesicles of 0.4–0.6 μm diameter. *N*-glycan GTs, GnTI-mRFP (A), GMII-mRFP (B), ST-YFP (C) were occasionally found in the smaller vesicles than the Golgi apparatus (indicated by arrows) similarly to AG GTs (Figures 1–3). Scale bars = 10 μm.

References

1. Hawes C, Satiat-Jeunemaitre B. The plant Golgi apparatus - going with the flow. Biochim Biophys Acta 2005;1744:465–517.
2. Day KJ, Staehelin LA, Glick BS. A three-stage model of Golgi structure and function. Histochem Cell Biol 2013;140:239–249.
3. Krause C, Richter S, Knöll C, Jürgens G. Plant secretome - From cellular process to biological activity. Biochim Biophys Acta 1834;2013:2429–2441.
4. Ding Y, Wang JJ, Stierhof Y-D, Robinson DG, Jiang L. Unconventional protein secretion. Trends Plant Sci 2012;17:606–615.
5. Cheng F, Zamski E, Guo W, Pharr DM, Williamson JD. Salicylic acid stimulates secretion of the normally symplastic enzyme mannitol dehydrogenase: a possible defense against mannitol-secreting fungal pathogens. Planta 2009;230:1093–1103.
6. Miki B, McHugh S. Selectable marker genes in transgenic plants: applications, alternatives and biosafety. J Biotechnol 2004;107:193–232.
7. Wang J, Ding Y, Wang J, Hillmer S, Miao Y, Lo SW, Wang X, Robinson DG, Jiang L. EXPO, an exocyst-positive organelle distinct from multivesicular endosomes and autophagosomes, mediates cytosol to cell wall exocytosis in Arabidopsis and tobacco cells. Plant Cell 2010;22:4009–4030.
8. De Graffenried CL, Bertozzi CR. The roles of enzyme localisation and complex formation in glycan assembly within the Golgi apparatus. Curr Opin Cell Biol 2004;16:356–363.
9. Hassinen A, Pujol FM, Kokkonen N, Pieters C, Kihlström M, Korhonen K, Kellokumpu S. Functional organization of the Golgi N- and O-glycosylation pathways involves pH-dependent complex formation that is impaired in cancer cells. J Biol Chem 2011;286:38329–38340.
10. Schoberer J, Liebminger E, Botchway SW, Strasser R, Hawes C. Time-resolved fluorescence imaging reveals differential interactions of N-glycan processing enzymes across the Golgi stack in planta. Plant Physiol 2013;161:1737–1754.
11. Seifert GJ, Roberts K. The biology of arabinogalactan proteins. Annu Rev Plant Biol 2007;58:137–161.
12. Knoch E, Dilokpimol A, Geshi N. Arabinogalactan proteins: focus on carbohydrate active enzymes. Front Plant Sci 2014;5:198. doi:10.3389/fpls.2014.00198.
13. Wu Y, Williams M, Bernard S, Driouich A, Showalter AM, Faik A. Functional identification of two nonredundant Arabidopsis alpha(1,2)fucosyltransferases specific to arabinogalactan proteins. J Biol Chem 2010;285:13638–13645.
14. Basu D, Liang Y, Liu X, Himmeldirk K, Faik A, Kieliszewski M, Held M, Showalter AM. Functional identification of a hydroxyproline-o-galactosyltransferase specific for arabinogalactan protein biosynthesis in Arabidopsis. J Biol Chem 2013;288:10132–10143.
15. Geshi N, Johansen JN, Dilokpimol A, Rolland A, Belcram K, Verger S, Kotake T, Tsumuraya Y, Kaneko S, Tryfona T, Dupree P, Scheller HV, Höfte H, Mouille G. A galactosyltransferase acting on arabinogalactan protein glycans is essential for embryo development in Arabidopsis. Plant J 2013;76:128–137.
16. Knoch E, Dilokpimol A, Tryfona T, Poulsen CP, Xiong G, Harholt J, Petersen BL, Ulvskov P, Hadi MZ, Kotake T, Tsumuraya Y, Pauly M, Dupree P, Geshi N. A β-glucuronosyltransferase from *Arabidopsis thaliana* involved in biosynthesis of type II arabinogalactan has a role in cell elongation during seedling growth. Plant J 2013;76:1016–1029.
17. Dilokpimol A, Geshi N. *Arabidopsis thaliana* glucuronosyltransferase in family GT14. Plant Signal Behav 2014;9:e28891.
18. Dilokpimol A, Poulsen CP, Vereb G, Kaneko S, Schulz A, Geshi N. Galactosyltransferases from *Arabidopsis thaliana* in the biosynthesis of type II arabinogalactan: molecular interaction enhances enzyme activity. BMC Plant Biol 2014;14:90. doi:10.1186/1471–2229–14–90.
19. Oka T, Saito F, Shimma Y, Yoko-o T, Nomura Y, Matsuoka K, Jigami Y. Characterization of endoplasmic reticulum-localized UDP-D-galactose: hydroxyproline O-galactosyltransferase using synthetic peptide substrates in Arabidopsis. Plant Physiol 2010;152:332–340.
20. Schoberer J, Vavra U, Stadlmann J, Hawes C, Mach L, Steinkellner H, Strasser R. Arginine/lysine residues in the cytoplasmic tail promote ER export of plant glycosylation enzymes. Traffic 2009;10:101–115.
21. Strasser R, Schoberer J, Jin C, Glössl J, Mach L, Steinkellner H. Molecular cloning and characterization of *Arabidopsis thaliana* Golgi alpha-mannosidase II, a key enzyme in the formation of complex N-glycans in plants. Plant J 2006;45:789–803.
22. Boevink P, Oparka K, Santa Cruz S, Martin B, Betteridge A, Hawes C. Stacks on tracks: the plant Golgi apparatus traffics on an actin/ER network. Plant J 1998;15:441–447.
23. Viotti C, Bubeck J, Stierhof Y-D, Krebs M, Langhans M, van den Berg W, van Dongen W, Richter S, Geldner N, Takano J, Jürgens G, de Vries SC, Robinson DG, Schumacher K. Endocytic and secretory traffic in Arabidopsis merge in the trans-Golgi network/early endosome, an independent and highly dynamic organelle. Plant Cell 2010;22:1344–1357.
24. Heazlewood JL, Durek P, Hummel J, Selbig J, Weckwerth W, Walther D, Schulze WX. PhosPhAt: a database of phosphorylation sites in *Arabidopsis thaliana* and a plant-specific phosphorylation site predictor. Nucleic Acids Res 2008;36:D1015–D1021.
25. Geldner N, Anders N, Wolters H, Keicher J, Kornberger W, Muller P, Delbarre A, Ueda T, Nakano A, Jürgens G. The Arabidopsis GNOM

ARF-GEF mediates endosomal recycling, auxin transport, and auxin-dependent plant growth. Cell 2003;112:219–230.
26. Grebe M, Xu J, Möbius W, Ueda T, Nakano A, Geuze HJ, Rook MB, Scheres B. Arabidopsis sterol endocytosis involves actin-mediated trafficking via ARA6-positive early endosomes. Curr Biol 2003;13:1378–1387.
27. Meckel T, Hurst AC, Thiel G, Homann U. Endocytosis against high turgor: intact guard cells of *Vicia faba* constitutively endocytose fluorescently labelled plasma membrane and GFP-tagged K-channel KAT1. Plant J 2004;39:182–193.
28. Samaj J, Read ND, Volkmann D, Menzel D, Baluska F. The endocytic network in plants. Trends Cell Biol 2005;15:425–433.
29. Dettmer J, Hong-hermesdorf A, Stierhof Y, Schumacher K. Vacuolar H + -ATPase activity is required for endocytic and secretory trafficking in Arabidopsis. Plant Cell 2006;18:715–730.
30. Tanaka H, Kitakura S, De Rycke R, De Groodt R, Friml J, De Rycke R, De Groodt R. Fluorescence imaging-based screen identifies ARF GEF component of early endosomal trafficking. Curr Biol 2009;19:391–397.
31. Reichardt I, Stierhof Y-D, Mayer U, Richter S, Schwarz H, Schumacher K, Jürgens G. Plant cytokinesis requires de novo secretory trafficking but not endocytosis. Curr Biol 2007;17:2047–2053.
32. Jaillais Y, Fobis-Loisy I, Miège C, Gaude T. Evidence for a sorting endosome in Arabidopsis root cells. Plant J 2008;53:237–247.
33. Choi S, Tamaki T, Ebine K, Uemura T, Ueda T, Nakano A. RABA members act in distinct steps of subcellular trafficking of the Flagellin Sensing2 receptor. Plant Cell 2013;25:1174–1187.
34. Langhans M, Förster S, Helmchen G, Robinson DG. Differential effects of the brefeldin A analogue (6R)-hydroxy-BFA in tobacco and Arabidopsis. J Exp Bot 2011;62:2949–2957.
35. Nebenführ A, Ritzenthaler C, Robinson DG. Brefeldin A: deciphering an enigmatic inhibitor of secretion. Plant Physiol 2002;130:1102–1108.
36. Hess MW, Müller M, Debbage PL, Vetterlein M, Pavelka M. Cryopreparation provides new insight into the effects of brefeldin A on the structure of the HepG2 golgi apparatus. J Struct Biol 2000;130:63–72.
37. Baldwin TC, Handford MG, Yuseff MI, Orellana A, Dupree P. Identification and characterization of GONST1, a golgi-localized GDP-mannose transporter in Arabidopsis. Plant Cell 2001;13:2283–2295.
38. Satiat-Jeunemaitre B, Cole L, Bourett T, Howard R, Hawes C. Brefeldin A effects in plant and fungal cells: something new about vesicle trafficking? J Microsc 1996;181:162–177.
39. Satiat-Jeunemaitre B, Hawes C. G.A.T.T. (a general agreement on traffic and transport) and brefeldin A in plant cells. Plant Cell 1994;6:463–467.
40. Tse YC, Mo B, Hillmer S, Zhao M, Lo SW, Robinson DG, Jiang L, Chung Y. Identification of multivesicular bodies as prevacuolar compartments in *Nicotiana tabacum* BY-2 cells. Plant Cell 2004;16: 672–693.
41. Lam SK, Cai Y, Tse YC, Wang J, Law AHY, Pimpl P, Chan HYE, Xia J, Jiang L. BFA-induced compartments from the Golgi apparatus and trans-Golgi network/early endosome are distinct in plant cells. Plant J 2009;60:865–881.
42. Schoberer J, Runions J, Steinkellner H, Strasser R, Hawes C, Osterrieder A. Sequential depletion and acquisition of proteins during Golgi stack disassembly and reformation. Traffic 2010;11:1429–1444.
43. Wang J, Cai Y, Miao Y, Lam SK, Jiang L. Wortmannin induces homotypic fusion of plant prevacuolar compartments. J Exp Bot 2009;60:3075–3083.
44. Qi X, Zheng H. Rab-A1c GTPase defines a population of the trans-Golgi network that is sensitive to endosidin1 during cytokinesis in Arabidopsis. Mol Plant 2013;6:847–859.
45. Gendre D, McFarlane HE, Johnson E, Mouille G, Sjödin A, Oh J, Levesque-Tremblay G, Watanabe Y, Samuels L, Bhalerao RP. Trans-golgi network localized ECHIDNA/Ypt interacting protein complex is required for the secretion of cell wall polysaccharides in Arabidopsis. Plant Cell 2013;25:2633–2646.
46. Scheuring D, Viotti C, Krüger F, Künzl F, Sturm S, Bubeck J, Hillmer S, Frigerio L, Robinson DG, Pimpl P, Schumacher K. Multivesicular bodies mature from the trans-golgi network/early endosome in Arabidopsis. Plant Cell 2011;23:3463–3481.
47. Strasser R. Challenges in O-glycan engineering of plants. Front Plant Sci 2012;3:218.
48. Robinson DG, Scheuring D, Naramoto S, Friml J. ARF1 localizes to the golgi and the trans-golgi network. Plant Cell 2011;23:846–849.
49. Earley KW, Haag JR, Pontes O, Opper K, Juehne T, Song K, Pikaard CS. Gateway-compatible vectors for plant functional genomics and proteomics. Plant J 2006;45:616–629.
50. Poulsen CP, Vereb G, Geshi N, Schulz A. Inhibition of cytoplasmic streaming by Cytochalasin D is superior to paraformaldehyde fixation for measuring FRET between fluorescent protein-tagged Golgi components. Cytometry A 2013;83:830–838.
51. Li J-F, Park E, von Arnim AG, Nebenführ A. The FAST technique: a simplified Agrobacterium-based transformation method for transient gene expression analysis in seedlings of Arabidopsis and other plant species. Plant Methods 2009;5:6.
52. Marion J, Bach L, Bellec Y, Meyer C, Gissot L, Faure J-D. Systematic analysis of protein subcellular localization and interaction using high-throughput transient transformation of Arabidopsis seedlings. Plant J 2008;56:169–179.
53. Liesche J, He H-X, Grimm B, Schulz A, Kühn C. Recycling of Solanum sucrose transporters expressed in yeast, tobacco, and in mature phloem sieve elements. Mol Plant 2010;3:1064–1074.
54. Schneider CA, Rasband WS, Eliceiri KW. NIH Image to ImageJ: 25 years of image analysis. Nat Methods 2012;9:671–675.